



**CONFORMATIONAL AND ELECTRONIC STUDY OF SEX  
PHEROMONE OF THE PINE PROCESSIONARY MOTH AND SOME  
RELATED DERIVATIVE COMPOUNDS WITH MODIFICATION IN  
THE POLAR GROUP.**

**E. R. Chamorro<sup>1</sup>, E. Benítez<sup>1</sup>, A. F. Sequeira<sup>1</sup> and N. M. Peruchena<sup>2</sup>**

<sup>1</sup> *Grupo de Investigación en Química Orgánica Biológica. Facultad Regional Resistencia,  
UTN. French 414, (H3500CHJ) Resistencia. Chaco. Argentina.*

**Email: quimobi@frre.utn.edu.ar**

<sup>2</sup> *Laboratorio de Estructura Molecular y Propiedades. Área de Química Física, FACENA,  
UNNE, Avda. Libertad 5460 (3400) Corrientes. Argentina.*

**Email: peruchen@exa.unne.edu.ar**

*Received July 1, 2008. In final form July 16, 2008*

---

**Abstract**

We report a conformational and electronic study of the sex pheromone of the pine processionary moth, *Thaumetopoea pytiocampa*, the (Z)-13-hexadecen-11-ynyl acetate (**1**) as well as the electronic properties of a few analogues, which were obtained by substitutions on the methyl group at the acetate function of the molecule (–OCO–R with R= –CH<sub>3</sub> (**1**); –CH<sub>2</sub>F (**2**); –CF<sub>3</sub> (**3**); –CH<sub>2</sub>CH<sub>3</sub> (**4**); –H (**5**); –CH<sub>2</sub>Cl (**6**) and –CCl<sub>3</sub> (**7**)). Analogue derivative (**8**) is also included, where –OCO is substituted by –SCO.

An exploratory study of the conformational energy surface at compound **1** was carried out varying the torsion angles around C<sub>1</sub>-O, ( $\varphi_1$ ); O-C(=O), ( $\varphi_2$ ) and C<sub>9</sub>-C<sub>10</sub>, ( $\varphi_3$ ) bonds, using semiempirical methods. The structural and electronic parameters as atomic charges and orbital energies were calculated. Total Electronic Charge Density maps were also determined for the pheromone molecule and their analogue derivatives. The results obtained at semiempirical level of theory with AM1 Hamiltonian were related to the stereoelectronic requirements necessary to produce the activity on biological receptor, by comparative electroantennogram responses, EAG.

**Keywords:** conformational analysis, charge density, AM1, theoretical calculations, molecular orbital theory, sex pheromone, semiempirical methods.

## Resumen

Nosotros presentamos un estudio conformacional y electrónico de la feromona sexual de la mariposa de la procesionaria del pino, *Thaumetopoea pytiocampa*, el acetato de (Z)-13-hexadecen-11-inilo (**1**) así como las propiedades electrónicas de unos pocos análogos obtenidos por sustitución sobre el grupo metilo en la función acetato de la molécula (-OCO-R con R= -CH<sub>3</sub> (**1**); -CH<sub>2</sub>F (**2**); -CF<sub>3</sub> (**3**); -CH<sub>2</sub>CH<sub>3</sub> (**4**); -H (**5**); -CH<sub>2</sub>Cl (**6**) y -CCl<sub>3</sub> (**7**)). También se incluye el análogo (**8**) donde -OCO se reemplazó por -SCO. Se realizó un estudio exploratorio de la superficie de energía conformacional en el compuesto **1**, empleando métodos semiempíricos, variando los ángulos de torsión alrededor de los enlaces C<sub>1</sub>-O, ( $\varphi_1$ ); O-C(=O), ( $\varphi_2$ ) y C<sub>9</sub>-C<sub>10</sub>, ( $\varphi_3$ ). Se calcularon parámetros estructurales y electrónicos como cargas atómicas y energías orbitales. También fueron determinados los mapas de densidad de carga electrónica total para la molécula de feromona y sus análogos. Los resultados obtenidos, a nivel semiempírico con Hamiltoniano AM1, fueron analizados en forma conjunta con los resultados obtenidos por electroantennografía, EAG, y relacionados con los requerimientos estereoelectrónicos necesarios para producir la actividad biológica.

**Palabras clave:** análisis conformacional, densidad de carga, AM1, cálculos teóricos, teoría de orbitales moleculares, feromonas sexuales, métodos semiempíricos.

---

## Introduction

The pheromones are chemical substances used by the organisms to transmit the information among individuals of the same specie. In this definition sex *attractors*, alarm and aggregation markers, territory markers as well as other substances that induce to a more complex control of social behavior and modulate other species' activities, are included [1].

The sex pheromones study of insects has a strong interest in the field of Ecological Chemistry. Modern methods use the Sex Confusion Technique (SCT) for pest control in the integral protection of plants and when dealing with forestry pests. This technique consists in distributing synthetic sex pheromone of one species evenly and in high doses over the crop to protect in order to modify the adult behavior and to diminish the probability of both sex meeting. In this emergent discipline there are many records about sex pheromones that have been used successfully in the control of destructive insects for agriculture [2,3].

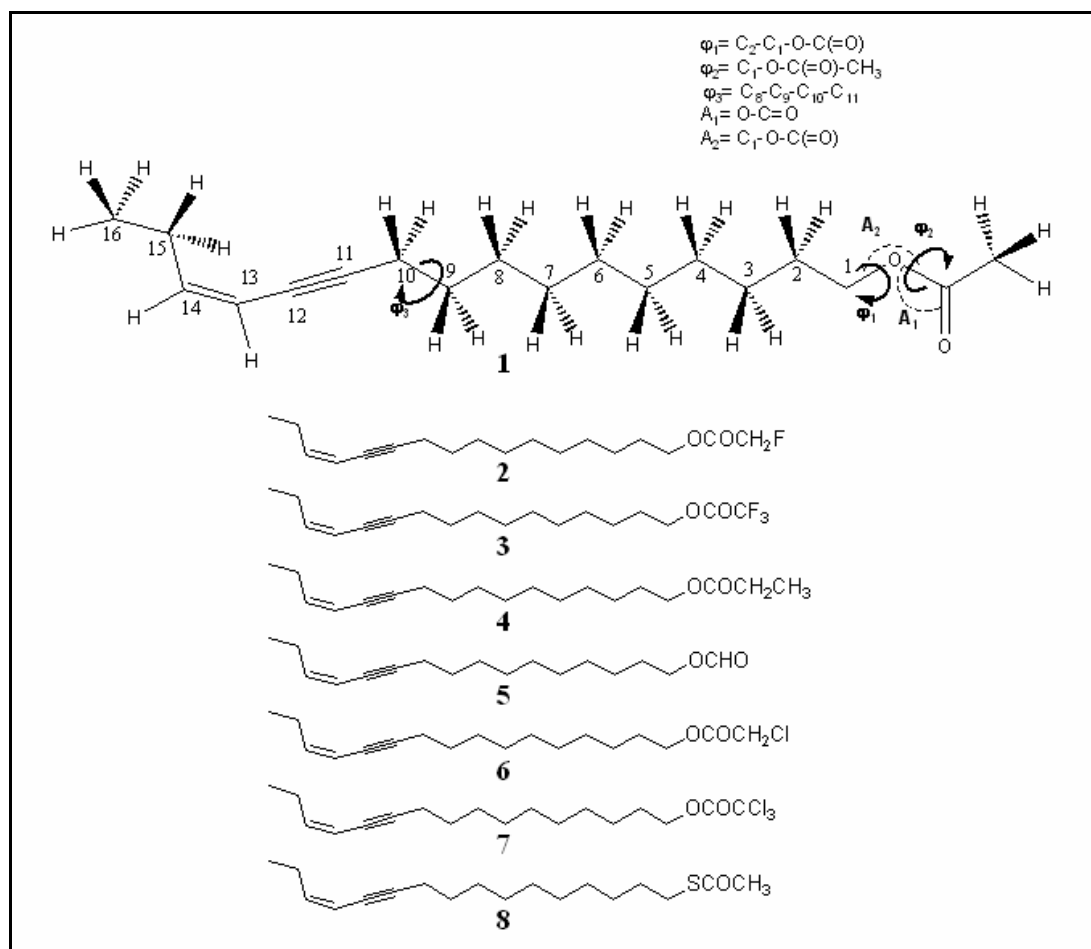
In a similar way, the use of synergistic analogues as well as anti-pheromones that block the chemical communication system -by irreversible activation of the specific receptors- would offer a supplementary alternative in this fight.

Odorant molecules and pheromones that are perceived by insects are small organic molecules (10–20 non-hydrogen atoms) and are usually hydrophobic and volatile [4]. They are detected by specialized sensillae in the antennae in which sensory neurons project their dendrites. In general, it is agreed that the perception process of the insect sex pheromone has strict structural requirements [5]. In addition, in the process of interaction between the substrate and the cell receptor, certain electronic requirements should also exist [6]. The interactions involved in the perception process may be electrostatic, hydrophilic, of van der Waals or of hydrogen bonds. All of them might contribute to configure a certain perception mechanism. It is also important to take into account the conformational flexibility of the receptor or its zones as well as the one of the substrate, in a way that one of them or both undergo the conformational changes required to establish the molecular recognition. The theoretical calculations have proved to be a valid alternative in the study of the biomolecules since they allow to predict the preferential conformations of the ligands by determining complete maps of the conformational surface, as well as to know the energetic differences among the several conformers [7-11]. In this context, it might be essential to know the conformational flexibility of the sex pheromone to understand the total attractant perception process and to clarify the underlying connection between the molecular structure and the biological activity. This knowledge will allow to design new synergic/inhibitor compounds able to increase/diminish the natural pheromone biological activity [12].

At the first stage of this work, calculations of the electronic structures were made to explore the hypersurface of the conformational potential energy of the major component of the sex pheromone of the pine processionary moth *Thaumetopoea pityocampa*, the (Z)-13-hexadecen-11-ynyl -acetate (Figure 1)[13a,b].

Three torsional angles  $\varphi_1$ ,  $\varphi_2$  and  $\varphi_3$  were considered relevant in this exploratory study (Scheme 1). Subsequently the electronic distribution is analyzed in the analogues obtained by structural modification of the molecule polar extreme.

In this molecule four zones can be distinguished whose possible changes may affect the activity or biological response of the compound: a) the enyne group:  $-\text{C}\equiv\text{C}-\text{C}(\text{H})=\text{C}(\text{H})-$ , b) the polar extreme  $-\text{OCO}-\text{R}$ , c) the length of the central hydrocarbonated chain and d) the side hydrocarbonated chain. To study a few analogues, besides compound **1**, seven additional (Z)-hexadecen-11-ynyl acetate derivatives were selected. These compounds have substitution of atoms in the acetate function. (Scheme1).



**Scheme 1.** A skeletal representation showing the numbering of the atoms and torsional angles for (Z)-13-hexadecen-11-ynyl acetate and its analogues, compounds **1-8**. The torsional angles are defined in terms of the atoms relevant in this work.

### Method of calculation

The exploratory study of the different molecular conformations of (Z)-13-hexadecen-11-ynyl acetate was carried out at RHF semi-empirical level with Hamiltonian AM1 (Austin Model 1) [14] and PM3 (Parametric Model 3) [15]. All the calculations were performed with the Gaussian03 program [16]. The conformations developed from the torsional behavior of three specific angles  $\varphi_1$ ,  $\varphi_2$  y  $\varphi_3$  which belong to  $C_1-O$ ,  $O-C(=O)$  and  $C_9-C_{10}$  bonds respectively, were analyzed. Starting from definite conformations: *g+*, *a* and *g-* (corresponding to  $60^\circ$ ,  $180^\circ$  and  $300^\circ$  respectively) in compound **1**, the conformational minima were obtained by total optimization of the rest the geometric parameters.

All the calculations of the structural and electronic parameters as well as the Total Electronic Charge Density (TECD) maps for the (Z)-13-hexadecen-11-ynyl acetate and its analogues, compounds **1-8**, were carried out at AM1 level, on optimized conformations. This method has been successfully used in the conformational study of other compounds [10-11]. The Mulliken Population Analysis [17] was used as it is implemented in the Gaussian 03 program. The graphic representation of the TECD maps and the frontier molecular orbitals, were performed with the Molekel 4.3 program [18].

## Results and discussion

From the different (*Z*)-13-hexadecen-11-ynyl acetate, **1**, molecular conformations, it is necessary to know which of them are essential to join the receptor located in the antenna. Thus, all the conformational possibilities should be analyzed

$$E = E (\varphi_1, \varphi_2, \chi_1, \dots, \chi_n, \varphi_3) \quad (1)$$

Where  $\chi_1, \dots, \chi_n$  identify the dihedral angles corresponding to the rotations round the  $Csp^3-Csp^3$  bonds of the central hydrocarbonated chain.

In an exploratory way we can consider the conformational behavior of the pheromone defined by three torsional angles  $\varphi_1$ :  $C_2-C_1-O-C(=O)$ ,  $\varphi_2$ :  $C_1-O-C(=O)-CH_3$  and  $\varphi_3$ :  $C_8-C_9-C_{10}-C_{11}$  (**Scheme 1**). Thus, the conformational study implies the analysis of the following potential energy hypersurface, (PEHS);

$$E = E (\varphi_1, \varphi_2, \varphi_3). \quad (2)$$

The rules of the Multi Configurational Dynamic Analysis (MCDA) [19] predict three theoretical positions of minimum-energy that arise from the rotation of the simple bonds,  $Csp^3-Csp^3$ . These positions correspond to  $\varphi_3 = 60^\circ$  (*gauche* +),  $\varphi_3 = 180^\circ$  (*anti*) and  $\varphi_3 = 300^\circ$  (*gauche* -). In a real molecule the minima *g*+, *a* and *g*- are in a scale of values, that is:  $0^\circ < g+ < 120^\circ$ , in the same way  $120^\circ < a < 240^\circ$  and  $240^\circ < g- < 360^\circ$ .

Thus, it is possible to partition of conformational problem in at least three potential energy surface, PES, of the kind:

$$E^{\varphi_3(g+)} = E (\varphi_1, \varphi_2) \quad (3)$$

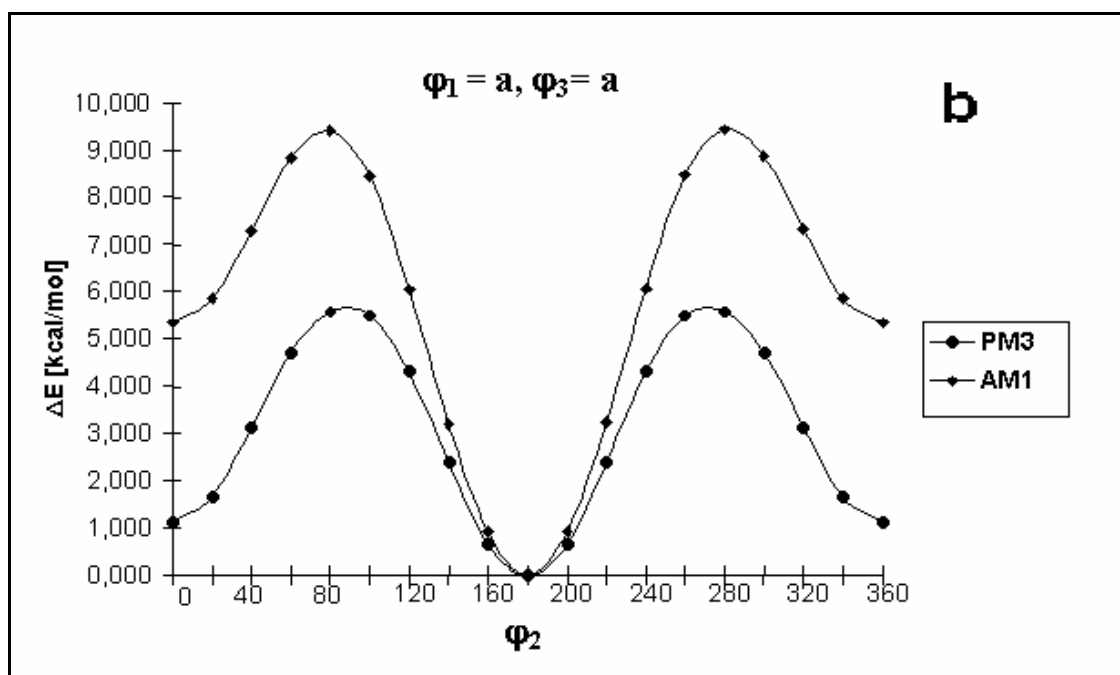
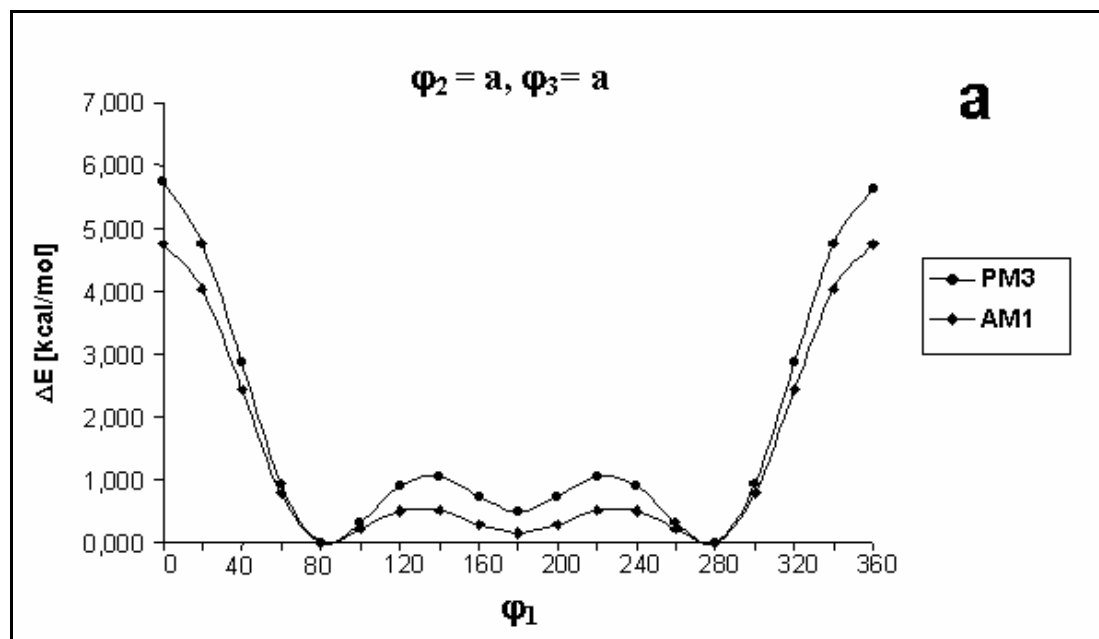
$$E^{\varphi_3(a)} = E (\varphi_1, \varphi_2) \quad (4)$$

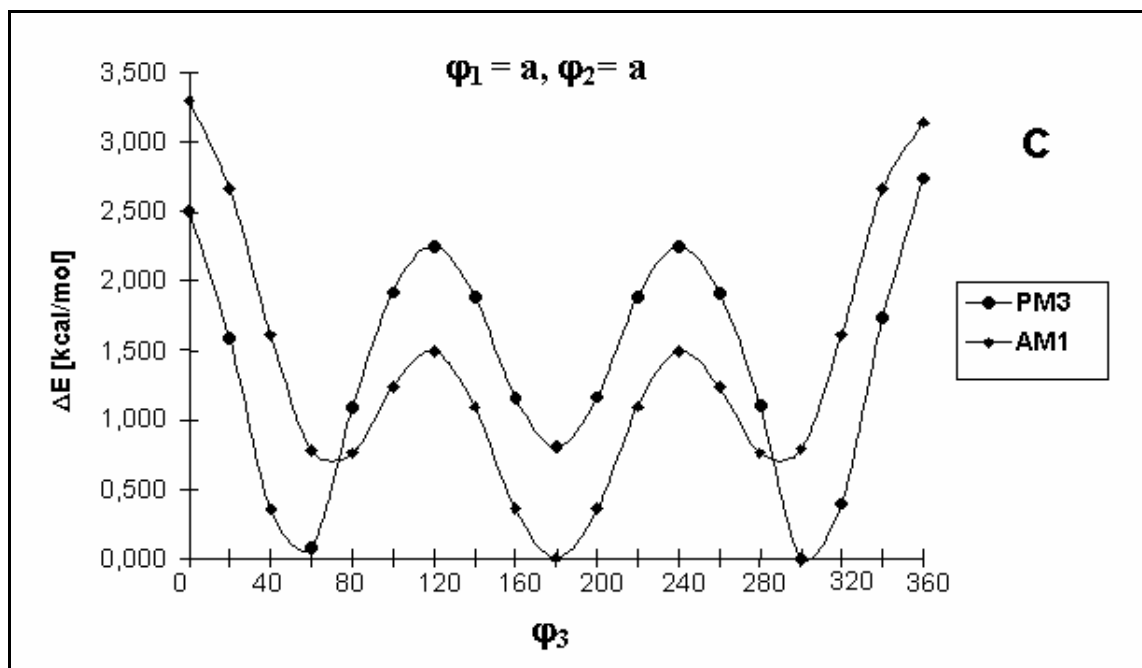
$$E^{\varphi_3(g-)} = E (\varphi_1, \varphi_2) \quad (5)$$

Where each equation represents a bi-dimensional potential energy surface (PES-2D) in which the enyne group is found in the three positions mentioned above,  $\varphi_3 = (g+, a, g-)$ .

Figure 1 shows the curves corresponding to the one-dimensional transversal surfaces, 1-D, according to which the conformational potential energy of the molecule varies when rotating  $\varphi_1$  (Fig. 1a),  $\varphi_2$  (Fig. 1b) and  $\varphi_3$  (Fig. 1c) from  $0^\circ$  to  $360^\circ$  obtained through AM1 and PM3 calculations. Each of these curves of potential energy are obtained varying the angle in question each  $20^\circ$ , keeping the other two torsion angles in  $180^\circ$  without any restriction on the rest of the parameters.

The first potential energy curve, Fig. 1a, shows three minima *g*+, *a* and *g*- and three maxima at  $0^\circ$ ,  $140^\circ$  and  $220^\circ$  respectively. The relative energy values for the maxima are higher in PM3 than those obtained by AM1 calculations. In AM1 and PM3 the energetic difference among the minima is very small, being lightly higher in this last one. Both methods predict conformational minima in *g*+ and *g*- (at  $80^\circ$  and  $280^\circ$ ) of less energy than the *anti* conformer. However, the energetic difference between the *gauche* and *anti* conformers in AM1, is minimal and can be considered mean.





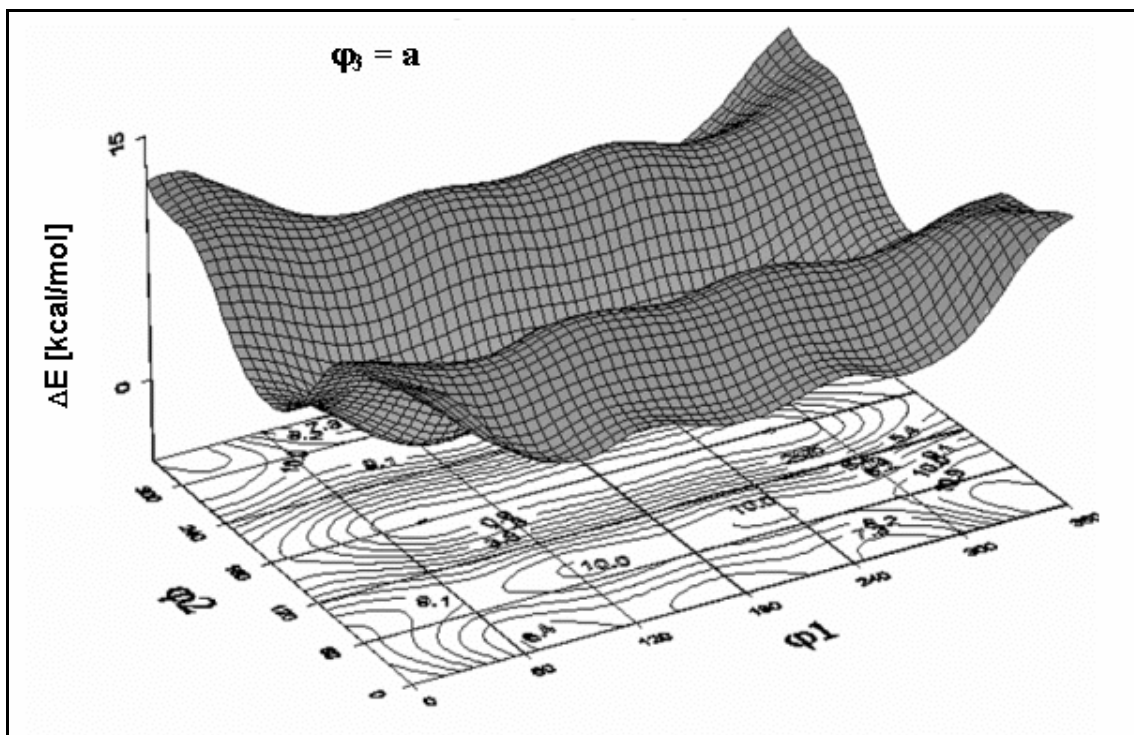
**Figure 1** Potential energy curves, PEC, obtained by rotation  $\varphi_1$  (Fig. 1a),  $\varphi_2$  (Fig. 1b) and  $\varphi_3$  (Fig. 1c) from  $0^\circ$  to  $360^\circ$ , obtained from AM1 and PM3 calculations.

Fig. 1b, corresponds to the rotation of the acetate group,  $Csp^2-Osp^3$ , shows the behavior of a typical bimodal curve with two minima and two maxima; the minima are found at  $0^\circ$  (*syn*) and  $180^\circ$  (*anti*), being this last one of lower energy. Both methods agree on the position of the minima and the maxima, but AM1 method shows a bigger difference of energy between the conformational minima, *syn* and *anti* (5.30 kcal/mol in AM1 vs. 1.2 kcal/mol in PM3) as well as between the maxima (*g+* and *g-*) and the *anti* energetic minimum.

Fig. 1c shows the molecule conformational behavior when the  $C_9-C_{10}$  bond adjacent to the enyne group rotates ( $-C\equiv C-C(H)=C(H)-$ ), keeping the dihedral angles  $\varphi_1$  and  $\varphi_2$  at  $180^\circ$ . The AM1 calculations show the three minima *g+*, *a* and *g-*, the global minimum corresponds to  $\varphi_3 = 180^\circ$ . The PM3 method also indicates three minimum energy positions but the *g+* and *g-* conformers are more stable than the *anti* conformer. In AM1 the values corresponding to the energetic maxima at  $0^\circ$  are higher than the maxima found at  $120^\circ$  and  $240^\circ$ , however, the PM3 method predicts higher relative energy values in these positions, with less energetic differences between the maxima. In AM1 the minima *g+* and *g-* are lightly shifted (to  $+70^\circ$  and  $-70^\circ$  respectively).

In order to carry out an exploratory study on the molecular structure of the (Z)-13-hexadecen-11-ynyl acetate, in this work the calculation of the Potential Energy Surfaces, and of the properties at a selected conformation obtained by total optimization is made, just like the rest of the calculations, with the AM1 method, for the pheromone as much as for its analogues. This method will be used subsequently in the evaluation of the oxygen atoms acceptor capacity in the acetate group to interact through hydrogen bonds [20].

Figures 2, 3 and 4 show the conformational potential energy surfaces, PES-2D, of **1** from AM1 calculations.



**Figure 2.** Conformational PES (landscape)  $E(\varphi_1, \varphi_2)$  with  $\varphi_3 = 180^\circ$  for (Z)-13-hexadecen-11-ynyl acetate obtained by AM1 calculations. Also, the contour map is shown at bottom.

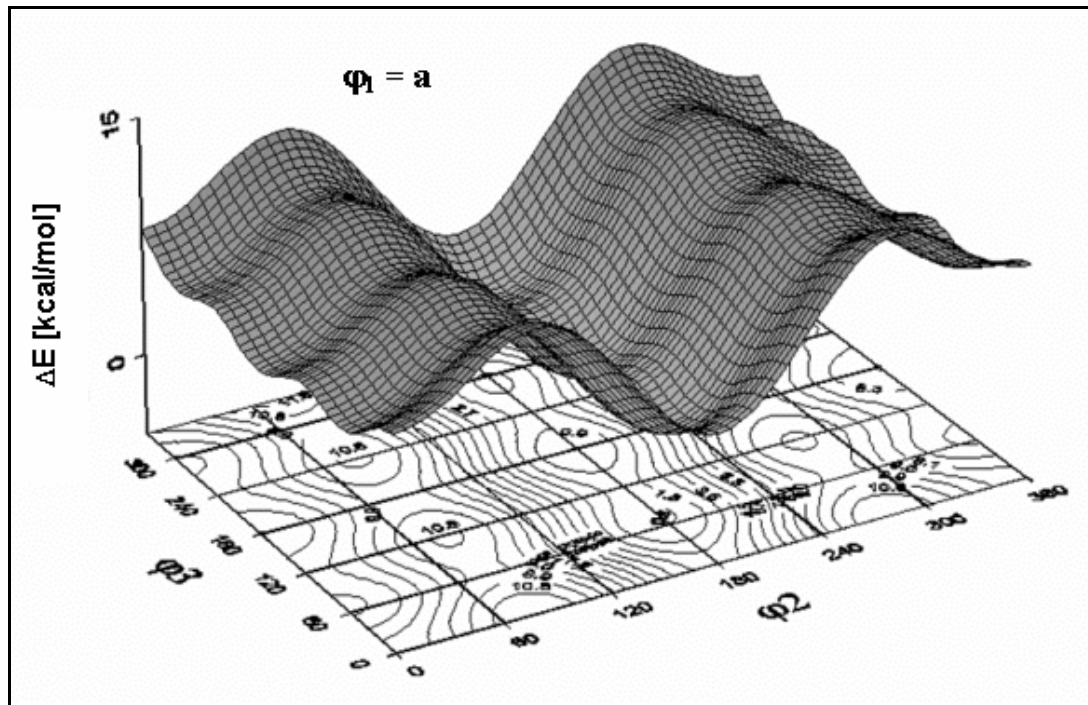


**Figure 3.** Conformational PES (landscape)  $E(\varphi_2, \varphi_3)$  with  $\varphi_1 = 180^\circ$  for (Z)-13-hexadecen-11-ynyl acetate obtained by AM1 calculations. Also, the contour map is shown at bottom.

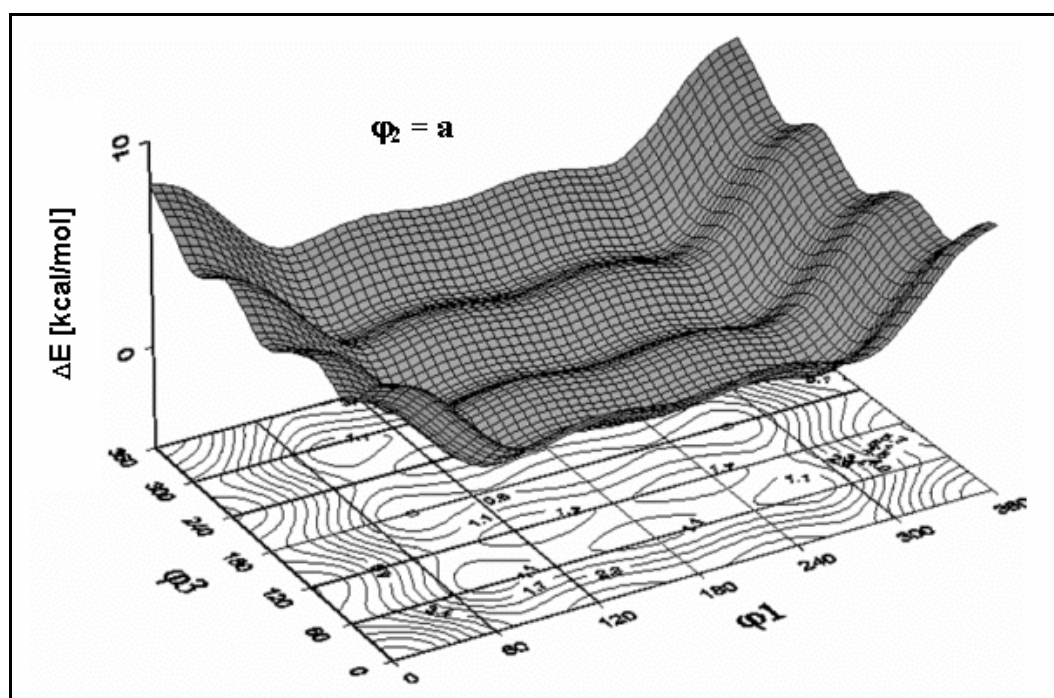


**Figure 4.** Conformational PES (landscape)  $E(\varphi_1, \varphi_3)$  with  $\varphi_2 = 180^\circ$  for (Z)-13-hexadecen-11-ynyl acetate obtained by AM1 calculations. Also, the contour map is shown at bottom.

These maps allow to visualize the conformational behavior of a compound when its spatial dispositions are fundamentally defined by two rotations [7]. The sweep of  $\varphi_1$  vs  $\varphi_2$  (every  $20^\circ$ ) keeping  $\varphi_3$  at  $180^\circ$  (Fig. 2), optimizing the rest parameters shows three conformational minima. The remaining two surfaces for  $\varphi_3$  at  $60^\circ$  and  $300^\circ$  are very similar (results not shown).

These minima were confirmed by calculations done with optimization of all the geometric parameters (Table 1).

In the same way, Figures 3 and 4 show the conformational potential energy surfaces, PES-2D, totally optimized, obtained through AM1 calculations for the  $\varphi_2$  vs.  $\varphi_3$  sweeps keeping  $\varphi_1$  in *anti* and  $\varphi_1$  vs.  $\varphi_3$  keeping  $\varphi_2$  in *anti* respectively.

In figure 3 it can be clearly observed that the 6 minima are located in the positions near to  $0^\circ$  and  $180^\circ$ , being these last ones energetically more favorable. The maxima are in the conformations *g+* and *g-* of  $\varphi_2$ , these last ones corresponding to values  $120^\circ$ ,  $240^\circ$  and  $0^\circ$  ( $360^\circ$ ) of  $\varphi_3$ . The PES shows  $\varphi_1$  vs.  $\varphi_3$  variation keeping  $\varphi_2$  in *anti* (Figure 4) allows to visualize in a clear way the 9 conformational minima predicted (*g+,g+*), (*a, g+*), (*g-, g+*); (*g+,a*), (*a,a*), (*g-, a*) and (*g+,g-*), (*a, g-*), (*g-,g-*); these were confirmed by total optimization.

Table 1 shows the values adopted by torsional angles  $\varphi_1$ ,  $\varphi_2$ ,  $\varphi_3$  after the total optimization process carried out with AM1 method over all the geometric parameters. The relative energies are also shown in kcal/mol for the different theoretical conformations (the 27 starting conformations are shown on the second column). The conformations reached after the total optimization process are indicated on the third column, with an arrow.

If three torsional angles  $\varphi_1$ ,  $\varphi_2$ ,  $\varphi_3$  and three possible positions for each of them (*gauche+*, *anti* and *gauche-*) are considered, they result in 27 theoretical conformations. Starting from these ones, 18 conformations or energetic minima were obtained, and it can be

clearly noted that the values of the torsion angles for  $\varphi_2$ , in the starting positions  $g^-$  and  $g^+$ , when optimized become near to  $0^\circ$  (between  $-6.57^\circ$  and  $6.54^\circ$ ). In Table 1 it also can be noticed that, as expected, for  $\varphi_2 = g^-$ , in 6 of the 9 starting conformations, conformational minima are not found.

The AM1 calculations reveal that the conformation with lower energy are  $(g^+, a, a)$  and  $(g^-, a, a)$ , this last one shows an energetic difference not statistically significant (0.02 kcal/mol). The results obtained for  $\varphi_1$  are in agreement with what it is observed in figure 1 where the positions  $g^+$  and  $g^-$  show the same energetic value.

**Table 1.** Torsional angles and energy gap obtained for the different conformations<sup>a)</sup> of (Z)-13-hexadecen-11-ynyl acetate from AM1 calculations.

N°	Conform. <sup>b)</sup>	$C_T \rightarrow (C_O)$	$\varphi_1 (^\circ)$	$\varphi_2 (^\circ)$	$\varphi_3 (^\circ)$	$\Delta E(\text{kcal/mol})$
1	$g^+ g^+ g^+$		86.87	6.47	70.10	6.369
2	$g^+ a g^+$		81.91	179.86	70.30	0.833
3	$g^+ g^- g^+$	3 $\rightarrow$ (2)	81.89	180.03	70.27	0.677
4	$a g^+ g^+$		181.37	0.17	70.16	6.696
5	$a a g^+$		180.50	180.04	70.20	1.477
6	$a g^- g^+$	6 $\rightarrow$ (4)	181.34	0.18	70.12	6.695
7	$g^- g^+ g^+$	7 $\rightarrow$ (8)	-98.30	179.75	70.27	1.514
8	$g^- a g^+$		-81.91	179.98	70.22	0.689
9	$g^- g^- g^+$		-86.87	-6.47	70.18	6.199
10	$g^+ g^+ a$		86.88	6.54	180.06	5.544
11	$g^+ a a$		81.83	179.93	179.93	0.000
12	$g^+ g^- a$	12 $\rightarrow$ (10)	86.90	6.50	180.09	5.544
13	$a g^+ a$		181.30	0.20	180.11	6.025
14	$a a a$		180.51	180.00	180.00	0.673
15	$a g^- a$	15 $\rightarrow$ (13)	181.29	0.17	180.10	6.025
16	$g^- g^+ a$	16 $\rightarrow$ (18)	-87.35	-5.69	179.94	5.550
17	$g^- a a$		-81.86	180.18	180.04	0.023
18	$g^- g^- a$		-86.84	-6.57	179.87	5.544
19	$g^+ g^+ g^-$		86.85	6.49	-70.14	6.199
20	$g^+ a g^-$		81.97	179.92	-70.26	0.689
21	$g^+ g^- g^-$	21 $\rightarrow$ (20)	81.90	180.00	-70.25	0.689
22	$a g^+ g^-$		181.30	0.19	-70.28	6.665
23	$a a g^-$		180.47	179.98	-70.24	1.324
24	$a g^- g^-$	24 $\rightarrow$ (22)	181.40	0.19	-70.29	6.665
25	$g^- g^+ g^-$	25 $\rightarrow$ (26)	-81.84	179.93	-67.50	0.541
26	$g^- a g^-$		-81.90	179.97	-70.31	0.677
27	$g^- g^- g^-$		-86.85	-6.49	-70.06	6.213

<sup>a)</sup> Theoretical conformations,  $C_T$  (idealized values) in the 27 starting positions.  $g$ , *gauche*;  $a$ , *anti*.

<sup>b)</sup> Optimized conformations,  $C_O$ . Between parenthesis are indicated the obtained conformations after the total optimization process.

Table 2a shows some structural parameters for compounds **1-8**, obtained through AM1 calculations, on totally optimized geometries, which are: distance between non-bonded atoms, C<sub>14</sub>...C(=O); the dihedral angles:  $\varphi_1$ ,  $\varphi_2$ ,  $\varphi_3$  and the bond angles, A<sub>1</sub> and A<sub>2</sub> (see Scheme 1). Observing this table it is evident that in the studied compounds, the structural differences do not relate significantly to the biological activity. The distances between C<sub>14</sub> and the carbon of the carbonyl group, and the dihedral angles  $\varphi_1$ ,  $\varphi_2$  and  $\varphi_3$  do not show major differences between the compounds **1-7**. Greater structural differences are found in compound **8** where the replacement of the oxygen atom by a sulfur atom one makes this distance increase ( $\Delta D = 0.48$  Å). In this compound it can be observed an increase in the value of the dihedral angle  $\varphi_1$  and an increase of the bond angle A<sub>1</sub>= S-C=O compared to the O-C=O, with a decrease of the angle A<sub>2</sub>.

**Table 2a.** Structural parameters for compounds **1-8**<sup>a)</sup>, obtained through AM1 calculations.

	D(C <sub>14</sub> ...C(=O)) <sup>b)</sup>	$\varphi_1$ (°)	$\varphi_2$ (°)	$\varphi_3$ (°)	A <sub>1</sub> (°)	A <sub>2</sub> (°)
<b>1</b>	17.713	81.83	179.93	179.93	118.76	118.03
<b>2</b>	17.710	81.43	179.95	179.95	119.71	117.75
<b>3</b>	17.684	80.30	180.35	179.95	122.74	117.54
<b>4</b>	17.927	81.94	178.69	179.93	118.71	118.03
<b>5</b>	17.712	81.95	179.80	179.94	119.93	118.49
<b>6</b>	17.696	80.65	180.87	179.93	119.57	117.87
<b>7</b>	17.694	80.58	180.20	179.94	119.86	117.47
<b>8</b>	18.193	110.17	180.94	179.96	122.93	106.15

a) The dihedral angles:  $\varphi_1$ ,  $\varphi_2$ ,  $\varphi_3$  and the bond angles: A<sub>1</sub> and A<sub>2</sub> are show in Scheme 1.

b) The distances are given in Å.

To analyze the stereoelectronic effects that define the complementarily between the active compound and the pheromone receptor, the atomic charges and the density of molecular electronic charge were calculated using Mulliken analysis, as set up in Gaussian03 program. Charge density isosurfaces to 0.002 au were represented by the pheromone and its analogues (see Figure 5); to this cut value, the TECD maps show the shape of the compounds studied. The substitution of H by F in compound **3** causes no significant structural modifications; however the abrupt decrease (of 78% - 79%) in the pheromonal activity in the mono and tri substituted compounds, should correspond to the different electronic distribution observed in these compounds. Many descriptors reflect simple molecular properties and thus can provide insight into the physicochemical nature of the biological activity under consideration.

Table 2b shows the atomic charges calculated on selected atoms of the polar region; the energies of the frontier orbitals HOMO and LUMO and their adjacent HOMO-1 and LUMO+1 molecular orbitals, as well as the difference among the energies of the HOMO-LUMO. The E<sub>HOMO</sub>, which represents HOMO energy, is the energy of the highest occupied molecular orbital, which is the opposite of LUMO energy, the energy of the lowest

unoccupied molecular orbital. These were selected as calculated electronic parameters. The greater  $E_{\text{HOMO}}$  is, the greater the electron-donating capability; conversely, the smaller  $E_{\text{LUMO}}$  is, the smaller the resistance to accept electrons. These variables are interpreted as measures of molecular reactivity and stability. As  $E_{\text{LUMO}}$  decreases (relative to other molecules), the molecule is less stable and more reactive. For  $E_{\text{HOMO}}$ , the situation is the opposite. In the fluorinated derivatives it can be noted that the HOMO orbital energies move to more negative values with scarce variation in the rest of the derivatives. The HOMO-1 orbital energies show no significant variations whereas in the energies of LUMO and LUMO+1 orbital greater variations are found. In the analogues where methyl group is replaced by an ethyl group (analogue 4) and by a hydrogen atom (analogue 5), the orbital energies and the differences of energy between HOMO and LUMO show similar values, but it can be clearly observed that the value of  $\Delta|\text{H-L}|$  is lower in the halogen derivative 7 and in halogen derivative 3. In table 2b the experimental biological activity data for the pheromone and its analogues taken from Camps and col. are also shown [21-23]. The recorded biological activity corresponds to bioassays carried out on the antenna of male adults in an electroantennogram, according to the technique described at Guerrero and col. [24].

**Table 2b.** Electronic parameters obtained through AM1 calculations and experimental biological activity data for compounds **1-8**<sup>a)</sup>.

	Biol. Act. <sup>b)</sup>	CHARGES				HOMO	LUMO	$\Delta \text{H-L} $	HOMO - 1	LUMO + 1
		%	C (=O)	O (=C)	-X-	C <sub>1</sub>	E(eV)	E(eV)	E(eV)	E(eV)
1	100.00	0.344	-0.388	-0.327	-0.103	-9.163	0.524	9.687	-10.346	1.136
2	21.11	0.312	-0.353	-0.327	-0.102	-9.177	0.511	9.788	-10.363	0.820
3	22.22	0.324	-0.314	-0.289	-0.108	-9.203	0.055	9.258	-10.394	0.125
4	86.66	0.346	-0.386	-0.328	-0.103	-9.162	0.525	9.687	-10.345	1.183
5	35.00	0.245	-0.388	-0.335	-0.106	-9.170	0.518	9.688	-10.354	1.130
6	6.66	0.346	-0.362	-0.317	-0.104	-9.168	0.293	9.461	-10.353	0.519
7	2.77	0.359	-0.327	-0.296	-0.105	-9.187	-0.684	8.503	-10.376	-0.284
8	8.58	0.107	-0.326	0.114	-0.397	-9.171	0.503	9.674	-9.901	0.516

<sup>a)</sup> With X= O for compounds **1-7** and X= S for compound **8**. Charges are given in ua.

<sup>b)</sup> Taken from references [21-23].

Figures 6, 7 and 8 show the LUMO, LUMO-1 and HOMO+1 molecular orbitals in the pheromone and its derivatives modified in the polar extreme. In the pheromone as well as in the studied analogues, the HOMO shows contributions from the atoms of region of the double and triple bond; their contribution are quite similar and thus are not shown in this work. In figure 6 the LUMO 3D shape in **1-8** compounds is shown. For example, the electron density

of the LUMO at an atom is a measure of the relative reactivity of the LUMO at that atom within a single molecule. In the monochlorine, **6**, trichlorine, **7**, and trifluoride, **3** derivative compounds and in the thioderivative, **8**, one it can be observed that the atomic contributions to LUMO come from the atoms of the polar region of the molecule (modified acetate group), whereas in the rest of the compounds this molecular orbital (MO) centers on the atoms of the double and triple bond region (Figure 6). In compound **6**, it can be noted a greater contribution (given by the values of the coefficient of the AOs in the MOs –values not shown–) of the carbon,  $Csp^3$ , from  $CH_2Cl$  moiety and chlorine  $p_y$ -orbital, with smaller contributions of the AOs centered on the other atom of carbon,  $Csp^2$ , and the both oxygen atoms.

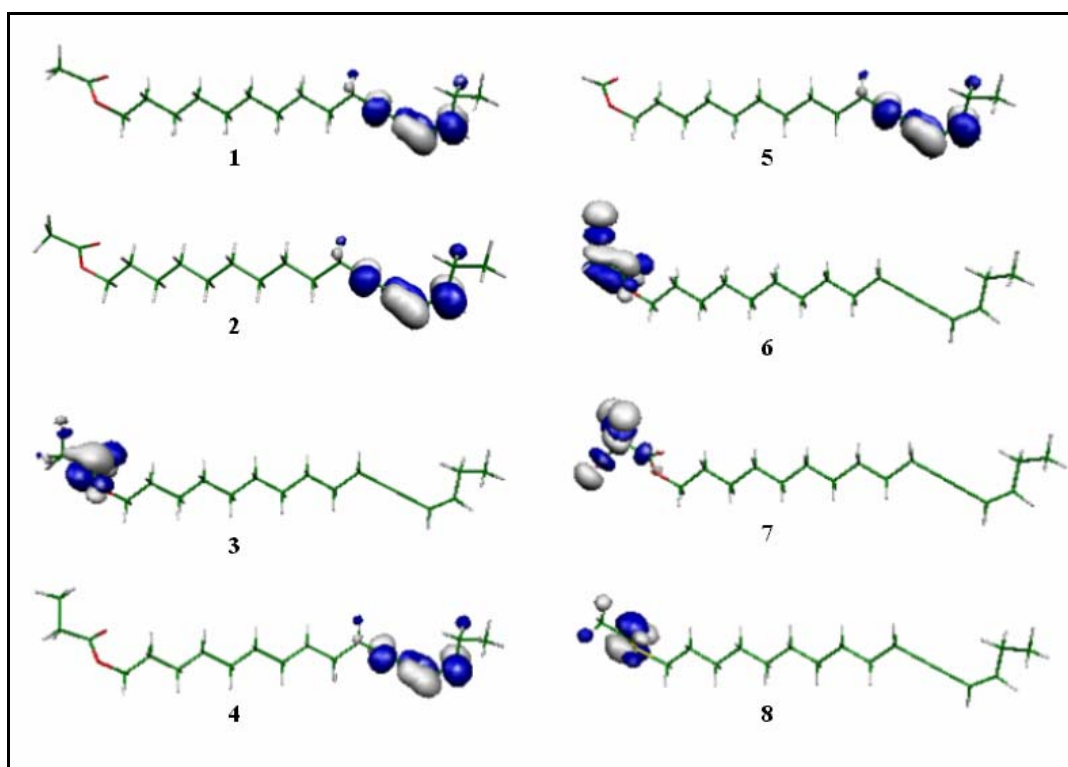


**Figure 6.** Low Unoccupied Molecular Orbital, LUMO, wave functions (isosurface to 0,05 ua) in compounds **1-8**.

Moreover, the AOs centered on the three chlorine atoms and on the carbon atom, in  $CCl_3$  moiety, contribute mainly to LUMO of the trichloride derivative, **7**, with small contributions from the AOs of the carbon from  $C=O$  group and oxygen of oxyester. In contraposition, the AOs of the F atoms hardly contribute to the LUMO of the trifluoride derivative. It is observed that, for this compound the major contribution comes from the AOs centered on the carbon and oxygen atoms. In the case of the thioderivative **8** the major contributions come from the AOs of the atoms of carbon, sulfur and oxygen at  $O=C-S$  moiety, with a lesser participation of the  $1s$  AOs of two hydrogen from methyl group.

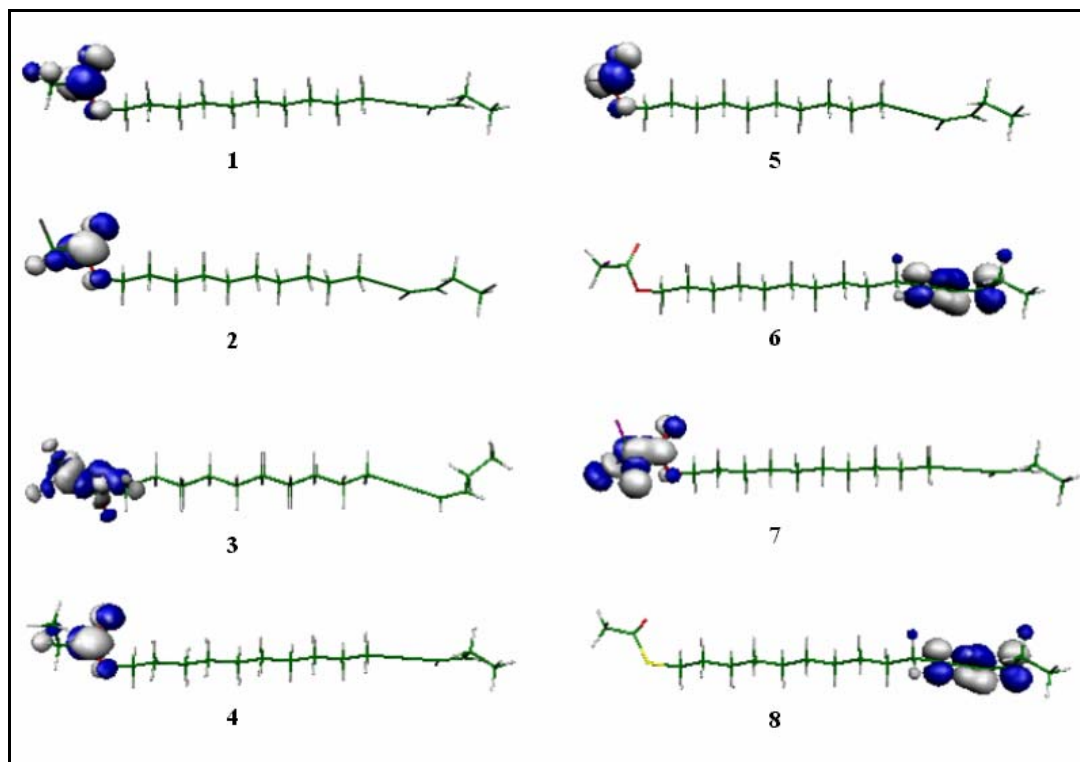


**Figure 7.** LUMO+1 wave functions (isosurface to 0.05 au) in compounds **1-8**.

On the other hand, LUMO+1 it is located in the polar region except for the monochloride analogue, **6**, and the thioanalogue, **8**, (see Figure 7); in these last two compounds, contributions from the atoms of the enyne group are observed. The major differences in the LUMO+1 are found in the trihalogenated derivatives, compounds **3** and **7**, at the same time that they are very different from one another, they show greater variations with regard to LUMO+1 in the pheromone. Compound **7** shows comparable contributions of two chlorine atoms and of both carbon atoms, followed by slight contributions of the AOs of the both oxygen atoms; whereas the LUMO+1 in compound **3** it can be observed greater contributions of carbons and lesser ones of the AOs corresponding to oxygen and fluorine atoms.

Figure 8 display the HOMO-1 in pheromone and analogues. However, with exception of the thioester, **8**, in the rest of the studied compounds, the HOMO-1 shows contributions from the atoms of region of the double and triple bond. In addition, their contributions are quite similar.

Since HOMO and LUMO energies and their adjoin orbital are related to the reactivity, it can be said that the halogenated compounds present greater energetic change at the LUMO in relation to the analogues modified by the replacement of Me by H and by Et in the polar region of the molecule. The analogue derivative of the natural sex pheromone that display greater activity inside of the studied series is the **4** compound, (86.66%) where a hydrogen atom from methyl group in acetate function is substituted by methyl, it is forming a propionate group of mayor volume. The energetic differences between gap ( $\Delta|H-L|$ ) in **1** and **4** is zero and between **1** and **5** compounds is quite similar ( $\Delta|H-L|_5 - \Delta|H-L|_1 = -0.001\text{eV}$ ), in contraposition the trichloride analogue, **7**, has the smaller biological activity with a decrease in  $\Delta|H-L|_7 = 8.503\text{eV}$ ; this is the difference of energy between gaps, between **1** and **7** compounds is of 1.184eV.

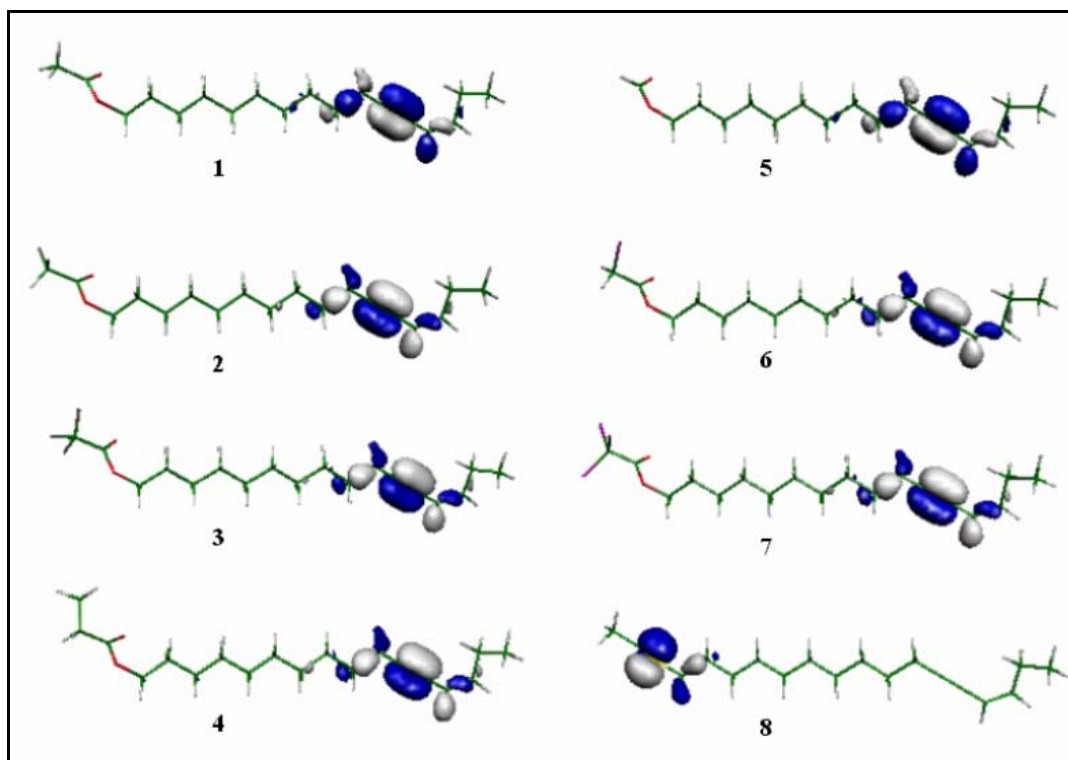


**Figure 8.** HOMO-1 wave functions (isosurface to 0.05 au) in compounds **1-8**.

On the other hand, the carbonylic and alkoxylic oxygen atoms, in the different compounds studied, are site of the highest concentrations of negative charge and it is assumed that these atoms shall be the preferred sites for an electrophilic attack. The values of the charges on the atoms of the polar region of the molecule show the effect of the replacement of hydrogen atoms by electronegative atoms. The halogen effect results in a decrease of the negative charge of the oxygen atom of the carbonyl group. This effect is not so marked in the oxygen atom of the alkoxylic group; however it can be observed a decrease of the charge on this oxygen for the trifluoro and trichloro derivatives.

In Table 2b, can be seen that the charge atomic on the carbonylic oxygen atoms shows the mayor variations in **3**, **7**, **2** and **6** analogues with decrease of 0.074au., 0.061 au., 0.035 au., and 0.026 au. respectively related to pheromone. Also, the thioester analogues shows a important diminution of the charge on oxygen at C=O group (0.062 au.) The results shows what compounds with electron withdrawing substituents (**2**, **3**, **6** and **7** analogues) takes electronic density from both oxygen atoms and these facts produce an important diminution of the negative charge; however note that as it were expressed before, the decrease in the atomic charge values is more notable in the oxygen atom at carbonyl group. Also, due to its greater electronegativity the fluorine atom produces a higher effect than the chlorine atom. As expected, the replacement of –O– by –S– results in a strong electronic effect due to lower electronegativity of the sulfur atom and greater polarizability of the C–S bond against C–O bond [25]. These changes are observed in table 2b for carbon and oxygen in carbonyl group and also in C<sub>1</sub> carbon atom.

In summary, the obtained results show that the biological activity is strongly related to the electronic distribution in the acyl group.

On the other hand, bearing in mind that there is an increase in size of the substituents due to the replacement of the methyl by ethyl groups – comparable to the replacement of three hydrogen atoms from methyl by a chlorine atom – and that there are no significant electronic changes between **1** and **4** to explain the decrease in the biological activity ( of the order of 15% ) with regard to the pheromone, it is reasonable to think that the chloride derivative size should contribute to produce a higher decrease of the biological activity than the one observed in the fluoride derivative. In consequence, it is necessary to consider that the size of the atoms (chlorine and sulfur) should also be an additional factor in relation to the biological activity in these compounds.

## Conclusions and perspectives

The results of the exploratory conformational analysis of (*Z*)-13-hexadecen-11-ynyl acetate, carried out at AM1 level considering three torsion angles:  $\varphi_1$  and  $\varphi_2$  located on the acetate group and  $\varphi_3$  close to the enyne group, show that the *gauche*<sup>+</sup> and *gauche*- conformations surrounding  $\varphi_1$  are highly preferred conformations, turning out to be (*g*<sup>+</sup>, *a*, *a*) and (*g*<sup>-</sup>, *a*, *a*) the conformations of lower energy. Also, the low energy gap between the different conformations suggest that a significant conformational interconversion can be take place in this compound. Only 18 conformations were obtained after the full optimization process. From the nine expected conformations for  $\varphi_3 = g^+$ , in AM1, only 6 were found when the full optimization was carried out. These six conformations can be divided in two groups according to the position (*syn* or *anti*) around the O-Csp<sup>2</sup> bond,  $\varphi_2$ , that connect the fragment 13-hexadecen-11-ynyl to the oxygen atom sp<sup>3</sup> of the acetate.

The differences observed in the biological activity for these analogues do not have any direct relation with the distance structural parameters, bond angles, dihedral angles, and molecular shape. Whereas, from the analysis of the electronic parameters, as the atomic charges, orbital energy and atomic contributions to the frontier molecular orbitals, it is evident that the replacement of H by electronegative atoms in the polar extreme of the pheromone molecule produces substantial changes in the electronic distribution; but the replacement of –CH<sub>3</sub> by –CH<sub>2</sub>CH<sub>3</sub> (**4**) and by –H (**5**) do not affect significantly the molecular electronic structure. The results obtained on the basis of the distribution of the electronic density are totally consistent with the ones observed experimentally in the laboratory essays, finding an abrupt decrease of the biological activity when the H of the methyl group are replaced by attractor atoms of electrons such as fluorine and chlorine. Also, the replacement of the oxygen atom by the sulfur atom in the –O–COCH<sub>3</sub> function produces changes in the structural and electronic parameters that result in a marked decrease of the biological activity.

The preliminary results obtained lead us to put forward that the decrease of the biological activity in the pheromone analogues with modifications in the acetate group, must be related to the electronic changes produced by the introduction of atoms or groups more electronegative, -analogues **2**, **3**, **6** and **7**- that decrease the electronic density on the oxygen of the carbonyl group. In other sex pheromones of insects that present an acetate group, it has been postulated that this group takes part in the binding, through hydrogen bonds, with the pheromone binding protein (PBP) [26,4]. A deeper electronic analysis based on Molecular Potential Electrostatic maps (MEPs), [27] and on electronic charge density maps, using the Theory of Atoms in Molecule, [28] at *ab initio* level is in progress in our laboratory.

This first stage of the study, at molecular level, of the natural sex pheromone of the processionary pine, *Thaumetopoea pytiocampa*, will be continued by the study of the electronic distribution in the analogues obtained by substitution in other regions of the molecule. It is expected that these works will help to clarify the current relationship between

the molecular electronic distribution in the pheromone and its analogues and the biological activity, so as to be able to design and propose a receptor model from the stereoelectronic requirements of the assayed analogues.

### Acknowledgements

The authors acknowledge to Angel Guerrero and Francisco Camps from Instituto de Ciencias Químicas y Ambientales from Barcelona, dependent on the CSIC from Spain for the experimental values of biological activity obtained by electroantennogram bioassays. The authors also thank to CONICET, Argentine by grant PIP 6337 and to SECYT UNNE and SECYT FRR UTN for financial support. N.M.P. is a career researcher of CONICET, Argentina.

### References

- [1]. Yan, F., Bengtsson, M. and Witzgall, P., *J. Chem. Ecol.*, **1999**, 2, 1343.
- [2]. a) Cichon, L.; Fernández, D., *Rompecabezas Tecnológico. Revista del Instituto Nacional de Tecnología Agropecuaria*, INTA, **2002**, 8, 33, 32 and references therein. b) Alfaro, R., *SAGPyA Forestal*, **2003**, 28, 11 and references therein.
- [3]. Renou, M.; A. Guerrero, *Annu. Rev. Entomol.*, **2000**, 48, 605.
- [4]. Pelosi, P. *J. Neurobiol.* **1996**, 30, 3.
- [5]. Manabe, S.; Takayanagi, H.; Nishino, C., *J. Chem. Ecol.*, **1983**, 9, 533.
- [6]. Manabe, S.; Nishino, C.; Matsushita, K., *J. Chem. Ecol.*, **1985**, 11, 1275.
- [7]. Leach, R. "A survey of Methods for searching the Conformational Space of Small and Medium-sized Molecules in Reviews in Computational Chemistry", K. B. Lipkowitz and D. B. Boyd, Eds., VCH Publishers, New York, **1990**, 1-55.
- [8]. Richards W. G., "Quantum Pharmacology" Chap. 13 and 15, 2<sup>nd</sup>. Ed. Butterworths, London, 1983.
- [9]. Enriz, R. D.; Rodríguez, A. M.; Jáuregui, E. A.; Pestchanker, M. J.; Giordano, O. S.; J. Guzmán *Drug. Des. Discovery*, **1994**, 11, 23.
- [10]. Fidanza, N. G.; Subiré, F. D.; Sosa, G.L.; Lobayan, R.M.; Enriz, R. D.; Peruchena, N.M., *J. Molec. Struct. (Theochem)*, **2001**, 543, 185.
- [11]. Fidanza, N. G.; Valiensi, J.P.; Peruchena, N.M.; *J. Molec. Struct.(Theochem)*, **2000**, 504, 59.
- [12]. a) Roelofs, W. L. *J. Insect. Physiol.*, **1969**, 17,. b) Roelofs, W. L.; Comeau, A. J. *J. Insect. Physiol.* **1971**, 17, 435.
- [13]. a) Guerrero, A.; Camps, F.; Coll, J.; Riba, M., J. Einhorn, Ch. Descoins and J. Lallemand, *Tetrahedron Lett.*, **1981**, 22(21), 2013. b) Quero C.; Malo E.A.; Fabriàs G.; Camps F.; Lucas P.; Renou M.; Guerrero A. *J. Chem. Ecol.*, **1997**, 23, 3,713
- [14]. Dewar, M.S.; Zoebisch, E.G.; Healy, E.F.; J.P. Stewart, *J. Am. Chem. Soc.* **1985**, 107, 3902.
- [15]. Stewart, J. J. P., *J. Comp. Chem.* **1989**, 10, 221.7.
- [16]. Frisch, M. J.; Trucks, G. W.; Schlegel, H. B.; Scuseria, G. E.; Robb, M.A.; Cheeseman, J. R.; Montgomery, J. A.; Jr., T. V.; Kudin, K. N.; Burant, J. C.; Millam, J. M.; Iyengar, S. S.; Tomasi, J.; Barone, V.; Mennucci, B.; Cossi, M.; Scalmani, G.; Rega, N.; Petersson, G. A.; Nakatsuji, H.; Hada, M.; Ehara, M.; Toyota, K.; Fukuda, R.;

- Hasegawa, J.; Ishida, M.; Nakajima, T.; Honda, Y.; Kitao, O.; Nakai, H.; Klene, M.; Li, X.; Knox, J. E.; Hratchian, H. P.; Cross, J. B.; Adamo, C.; Jaramillo, J.; Gomperts, R.; Stratmann, R. E.; Yazyev, O.; Austin, A. J.; Cammi, R.; Pomelli, C.; Ochterski, J. W.; Ayala, P. Y.; Morokuma, K.; Voth, G. A.; Salvador, P.; Dannenberg, J. J.; Zakrzewski, G.; Dapprich, S.; Daniels, A. D.; Strain, M. C.; Farkas, O.; Malick, D. K.; Rabuck, A. D.; Raghavachari, K.; Foresman, J. B.; Ortiz, J. V.; Cui, Q.; Baboul, A. G.; Clifford, S.; Cioslowski, J.; Stefanov, B. B.; Liu, G.; Liashenko, A.; Piskorz, P.; Komaromi, I.; Martin, R. L.; Fox, D. J.; Keith, T.; Al-Laham, M. A.; Peng, C. Y.; Nanayakkara, A.; Challacombe, M.; Gill, P. M. W.; Johnson, B.; Chen, W.; Wong, M. W.; Gonzalez, C.; Pople, J. A. *Gaussian 03*, Revision D.01; Gaussian, Inc.: Wallingford CT, 2004.
- [17]. Mulliken R. S., *J. Chem. Phys.* **1962**, *36*, 3428.
- [18]. *MOLEKEL* 4.3, P. Flükiger, H.P. Lüthi, S. Portmann, J. Weber, Swiss Center for Scientific Computing, Manno (Switzerland), 2000-2002.
- [19]. Csizmadia, I. G. *Multidimensional theoretical stereochemistry and Conformational potential energy surface topology, new theoretical concepts for understanding Organic Reactions*. Reidel, Dordrecht, The Netherlands, 1989.
- [20]. Results in preparation.
- [21]. Camps, F.; Fabriás, G.; Gasol, V.; Guerrero, A.; Hernandez, R.; Montoya, R., *J. Chem. Ecol.*, **1988**, *14*, 1331.
- [22]. Camps, F.; Fabriás, G.; Guerrero, A., *Tetrahedron*, **1986**, *42*, 3623.
- [23]. Camps, F.; Gasol, V.; Guerrero, A., *J. Chem. Ecol.*, **1990**, *16*, 1155.
- [24]. Guerrero, A.; Murgo, R.; Martorell, X., *Physiol. Entomol.*, **1986**, *11*, 273.
- [25]. Hansson, B. S.; Ochieng, S. A.; Wellmar, U.; Jonsson, S. and Liljefors, T., *Physiol. Entomol.*, **1996**, *21*, 275.
- [26]. a) Tegoni, M., Campanacci, V. and Cambillau, C., *Trends in Biochem. Scie.*, **2004**, b) Sandler, B.H., Nikonova, L., Leal, W.S., and Clardy, J. *Chem. Biol.* **2000**, *7*, 143.
- [27]. Politzer, P.; Truhlar, D. G., *Chemical Applications of Atomic and Molecular Electrostatic Potentials*, Plenum Press, New York, 1981.
- [28]. Bader, R.F.W. *"ATOMS IN MOLECULES. A quantum Theory"* Clarendon Press. Oxford Science Publications, 1990.